Journal of Materials Chemistry B

ROYAL SOCIETY OF CHEMISTRY

PAPER

View Article Online
View Journal | View Issue

Cite this: J. Mater. Chem. B, 2025, 13, 7744

Low-cost, robust, and transportable devices based on Cu(I)–I cluster hybrid luminescent compounds as tetracycline sensors for contaminated waters†

Elena De La Rubia,[a] Ricardo Garsed,[a] Fernando Aguilar-Galindo,[bd] Andrea García-Hernán,[a] Gines Lifante-Pedrola[c] and Pilar Amo-Ochoa *[ad]

Submicron particles of $[Cu_4I_6(pr\text{-}ted)_2]$ (pr-ted = 1-propyl-1,4-diazabicyclo[2.2.2]octan-1-ium) are easy to synthesize in one step under mild conditions. Additionally, they exhibit strong emission at 530 nm, high photoluminescence quantum yield, and excellent thermal (250 °C) and water stability (pH = 4–9). These properties make them a promising candidate for studying luminescence responses to external stimuli, potentially serving as a chemical sensor. Furthermore, their size and morphology make it possible to obtain stable suspensions in ethanol and water, which are extremely useful for subsequent processing. Indeed, submicrometric $[Cu_4I_6(pr\text{-}ted)_2]$ particles in deionized water and real river water suspensions can be used to efficiently detect tetracycline (TC) *via* photoinduced electron transfer, resulting in a detectable fluorescence quenching. It features a low detection limit of 1.18 nM (0.52 ppb) and the reversible quenching of the emission demonstrates recyclability for over 30 cycles. The detection process is unaffected by other antibiotics, including sulfamethazine (SMZ), chloramphenicol (CAP), and ornidazole (ORN). Effective TC detection is supported by the theoretical computations of the energy bands of TC antibiotic and $[Cu_4I_6(pr\text{-}ted)_2]$, indicating a good match between their energy bands, which aligns with the fluorescence quenching observed. As a proof of concept, the material has been further processed into various formats – such as pellets, paper strips, fiberglass, polylactic acid (PLA) composite films, and 3D-printed composite meshes using commercial photosensitive resins-for their practical application as robust, high sensitivity, rapid on–off response, and cost-effective tetracycline water sensor devices.

Received 17th February 2025,
Accepted 14th May 2025

DOI: 10.1039/d5tb00353a

rsc.li/materials-b

1. Introduction

Considerable attention has been devoted to developing sensors capable of detecting environmentally relevant species or physical changes. These sensors serve various purposes, including monitoring harmful substances affecting human health and detecting pressure or temperature changes, among others.[1–3] They hold promise for applications in water or food treatments, memory devices, and motion or damage sensors, among others.[4–7] For instance, the detection of antibiotics is crucial due to the presence of antibiotic residues, which pose serious threats to public health.[8,9] While traditional methods like Raman spectroscopy, high-performance liquid chromatography, and gas chromatography coupled with mass spectrometry are efficient and sensitive, they suffer from drawbacks such as being time-consuming, requiring specialized expertise, high costs, and inconvenience in portability. Although rapid colorimetric methods have emerged for identifying antibiotics in food and milk by inhibiting bacterial growth, to our knowledge, there are currently no effective detectors for antibiotics in water available on the market.[10]

Among the various detection techniques developed, luminescent stimuli-responsive materials based on coordination compounds are promising candidates for chemical sensing. These materials offer advantages like simple preparation, high sensitivity, cost-effectiveness, rapid operation, selectivity, and ease of use.[11–14]

Despite a significant increase in the number of luminescent compounds responsive to various stimuli reported over the past

[a] Dpto. de Química Inorgánica, Universidad Autónoma de Madrid, 28049, Madrid, Spain. E-mail: pilar.amo@uam.es
[b] Dpto. Química, Universidad Autónoma de Madrid, 28049, Madrid, Spain
[c] Dpto. de Física de Materiales, Universidad Autónoma de Madrid, 28049, Madrid, Spain
[d] Institute for Advanced Research in Chemical Sciences (IAdChem), Universidad Autónoma de Madrid, 28049, Madrid, Spain

† Electronic supplementary information (ESI) available: Characterization of the 1-propyl-1,4-diazabicyclo[2.2.2]octan-1-ium (pr-ted) ligand, and the submicrometric $[Cu_4I_6(pr\text{-}ted)_2]$ particles. Water stability characterization of submicrometric $[Cu_4I_6(pr\text{-}ted)_2]$ particles as a function of time and pH. Sensing *versus* tetracycline. Sensor selectivity and recyclability characterization. DFT calculations. Fluorescence quenching mechanism to TC. Portable device characterization. (PDF). See DOI: https://doi.org/10.1039/d5tb00353a

decade,[15,16] several limitations persist in the existing body of research. Firstly, many studies primarily focus on compounds derived from lanthanides.[17,18] Secondly, most research emphasizes changes in emission in response to specific stimuli, without advancing towards the development of cost-effective, robust, sensitive, and user-friendly devices.[19–22] Thirdly, comprehensive studies investigating the underlying mechanisms of luminescence quenching in these materials remain relatively scarce.[23–25] Therefore, there is a pressing need for new research that explores alternative, more abundant, and less toxic metallic elements, investigates easily processable materials, and delves deeper into the mechanisms. Such efforts are crucial to guiding the development of stimuli-responsive materials with optimized properties.

Copper(I) coordination compounds are very attractive from the viewpoint of effective utilization of common metals since copper is a more abundant, and inexpensive resource and its extraction generates less toxic waste than lanthanide mining.[26–28] Additionally, these compounds exhibit interesting features due to their lability and high flexibility in metal–metal, and metal–ligand coordination bonds.[29,30] These properties make them advantageous for chromic materials since they exhibit changes in luminescence in response to external stimuli such as temperature, mechanical force, or the presence of vapors or ions.[3,31,32] Traditionally mononuclear or multinuclear Cu(I) complexes exhibit metal-to-ligand charge transfer (MLCT) and/or intraligand π–π* emission properties and can display characteristic luminescence originating from the intracore d–p electronic transition, commonly referred to as cluster-centered (CC) transition.[33,34]

Recently, a new type of Cu(I)–I cluster-based hybrid with a special all-in-one structure, containing ionic and covalent bonds between the inorganic core and organic ligands, has been reported.[35–37] This new kind of Cu(I)–I-based hybrid is composed of isolated clusters possessing high structural stability (i) and efficient phosphorescence due to the strong spin–orbital coupling in the cluster (ii). Stability is particularly important for a luminescent sensor in practical applications as detection typically occurs under various complex environments, including humid air, acidic or basic conditions, or at elevated temperatures. The high luminescence of the hybrid cluster, along with its wide Stokes shift, is essential for visual sensor applications.

In this research we have chosen the $[Cu_4I_6(pr\text{-}ted)_2]$ (pr-ted = 1-Propyl-1,4-diazabicyclo[2.2.2]octan-1-ium) as a Cu(I)–I cluster-based hybrid compound.[35] This compound exhibits remarkable features, including an intense luminescence emission at 530 nm, an almost 100% photoluminescent quantum yield, high thermal stability (exceeding 250 °C), and the ability to be synthesized in various morphologies and sizes, including submicron-particles with spherical shapes ranging from 200 to 300 nm in diameter. These characteristics make it a promising candidate for the development of luminescent inks. The small particle size enables the formation of stable suspensions that ease the processing of the compound into robust, cost-effective, and portable composite materials. In this study, pellets and composite devices based on paper, fiberglass, and polylactic acid (PLA) were developed, along with the creation of 3D objects using photosensitive resins. The findings demonstrate the high sensitivity and robustness of the devices and their rapid response to tetracycline in water. The results obtained are significant compared to most studies published to date (Table 1).

2. Experimental details

2.1 Materials and methods

The chemical composition of the samples was determined by elemental analysis using the LECO CHNS-932 elemental analyzer from the Eltra company. ^{1}H-NMR spectra were recorded using a Bruker Advance III-HD Nanobay 500 MHz spectrometer. A PerkinElmer 100 spectrophotometer with ATR sampling was used to record IR spectra. X-ray powder diffraction (PXRD) measurements were carried out with a Bruker D8 Advance A25 diffractometer with a Cu Kα X-ray radiation source, a PSD-XE detector with positive energy discrimination, and optical recognition of components (DAVINCI). A Hitachi S-3000N SEM-EDX microscope was employed to obtain images of the synthesized $[Cu_4I_6(pr\text{-}ted)_2]$ particles determining the size and composition of the samples. The particle size of $[Cu_4I_6(pr\text{-}ted)_2]$ particles was also determined through dynamic light scattering (DLS). A VASCO particle size analyzer from Cordouan Technologies has been used. Thermogravimetric analysis (TGA) was performed with differential thermal analysis (DTA) using a TA Instruments Q500 thermobalance oven containing a Pt sample holder. Emission measurements were recorded on a photoluminescence spectrometer FLS 1000 from Edinburgh Instruments. The emission spectra of $[Cu_4I_6(pr\text{-}ted)_2]$ particles in aqueous

Table 1 Comparison of K_{sv}, recyclability, and LOD obtained in this work for the detection of TC in aqueous media with other published data

Coordination compounds	K_{sv} (M^{-1})	LOD (nM)	Recyclability
MOF $[Tb(HL)L(H_2O)]_n$ (H_2L = salicylic acid)[38]	1.39×10^4	2.77	30
MOF Zr/Cit-Eu (Cit = Citrate)[39]	—	3.90	n.r.
MOF $[Cd(H_2L)\cdot(H_2O)_2]$ (H_2L = 5-methyl-1,3-dimethylphosphonic acid)[40]	1.29×10^4	4.27	n.r.
MOF HZIF-8[41]	—	6.56	n.r.
MOF Eu-TCPE (TCPE = tetrakis(4-carboxyphenyl)ethylene)[42]	1.49×10^5	14.0	n.r.
$[Cd(opda)(tib)]\cdot H_2O$ phenylenediacetates (H_2pda) and 1,3,5-tris(1-imidazolyl)benzene (tib)[43]	3.85×10^5	560	5
$[Zn(1,1'\text{-bbi})(C_2O_4)]_n$ (1,1′-bbi = 1,1′-(1,4-butanediyl)bis(imidazole))[44]	3.48×10^4	860	5
$[Cu_4I_4(ETBT)_4]$[45] (ETBT = 2-ethylbenzo[d]thiazole)	3.23×10^3	4550	5
Submicrometric $[Cu_4I_6(pr\text{-}ted)_2]$ particles in deionized/river water	4.35×10^4/4.11×10^4	1.2/1.9	30

n.r. = not reported.

suspension were obtained using an FS5 spectrofluorimeter (Edinburgh Instruments) at room temperature. The luminescence of the samples was induced by UV-light excitation using an arc Xe lamp. Emission and excitation spectra were obtained using monochromators with Czerny–Turner design with a double grating turret, flat grating for precise focusing at all wavelengths, and minimal stray light. All the data obtained in the TC detection experiments were measured three times, using a quartz cuvette. Sonication was done in a Transsonic Digital S unit, Elma, ultrasonic bath. In this work, all samples were sonicated at 24 °C and 60% power. An MPW-350R centrifuge was used for sample centrifugation. Theoretical calculations were performed in the framework of density functional theory (DFT) with the Vienna *ab initio* simulation package (VASP),[46] which imposes periodic boundary conditions (PBCs), allowing for an appropriate description of the material. The electron density was expanded on a plane wave basis with a kinetic energy cutoff of 450 eV, while the interaction between electrons and nuclei was described with the projected augmented wave (PAW) pseudopotentials from the VASP database. Reciprocal space was sampled using the G point. We considered the electron density as converged when the difference between two steps in the self-consistent field was lower than 10–5 eV. Structures were considered as converged when all the Hellman–Feynman forces were lower than 0.01 eV $Å^{-1}$. Geometry optimizations were performed with the OPTPBE functional,[47,48] which allows for a correct description of weak interactions (*i.e.* van der Waals forces). On the top of the optimized structures, single-point calculations using the hybrid Heyd–Scuseria–Ernzerhof HSE06 functional[49] were used, which is known to provide good band gap values in solid-state calculations. Uniaxial pressure was applied using a Model 4350 CARVER manual bench-top pellet press. An ELEGOO Mars 2 Pro 3D printer was employed to fabricate a 5 cm × 5 cm mesh with a 1 mm height using the ELEGOO Standard Photopolymer Resin, which was diluted with ethanol to decrease viscosity and enhance flow properties during printing; the resin–ethanol mixture was poured into the printer's tank, where controlled UV light exposure cured the mesh layer by layer according to the printer's settings, achieving a precise and stable network structure.

All reagents were used as purchased from commercial suppliers. Triethylenediamine (≥99%), 1-bromopropane (≥99%), polyvinylpyrrolidone (PVP, CAS: 9003-39-8), and cuprous iodide (≥98%) were supplied by Sigma Aldrich. Ethanol (≥99.9%), was purchased from Scharlau. The supplier for acetone (≥99.8%) is Carlo Erba. KI (≥99%) was supplied by Labkem. The antibiotics used in this work are sulfamethazine (SMZ, 99.0–101.0%, CAS: 57-68-1), chloramphenicol (CAP, 98%, CAS: 56-75-7), tetracycline (TC, 98.0–102.0%, CAS: 60-54-8) and ornidazole (ORN, CAS: 16773-42-5), all purchased at Sigma Aldrich. The biodegradable organic polymer used was polylactic acid (PLA, CAS: 459-898-81), which was purchased from Sigma Aldrich. The solvent used for processing $[Cu_4I_6(pr\text{-}ted)_2]$@PLA1% was chloroform ($CHCl_3$, 99.8%, CAS: 67-66-3), which was obtained from Thermo Fisher Scientific. Standard Photopolymer Resin was purchased from ELEGOO.

2.2 Synthesis

2.2.1 Optimized synthesis of pr-ted. Although the synthesis of the 1-propyl-1,4-diazabicyclo[2.2.2]octan-1-ium (pr-ted) ligand has been previously published,[35,50] we have optimized the process: 2.24 g (20 mmol) of triethylenediamine (ted) are introduced inside a Falcon tube and dissolved in 10 mL of acetone. 1.82 mL (20 mmol) of 1-bromopropane are then added dropwise. The content of the Falcon tube is left stirring overnight. The next day, a solid white phase and a liquid colourless phase can be seen. The liquid phase is removed by using a Pasteur pipette and, after washing the solid with 2 mL of acetone, it was left to dry inside a vacuum desiccator overnight. Yields between 91–96% have been obtained for this reaction. ^{1}H-NMR (300 MHz, CD_3CN): δ 3.29 (m, 6H), 3.16 (m, 2H), 3.03 (dd, J = 8.9, 6.0 Hz, 6H), 1.68 (m, 2H), 0.91 (t, J = 7.3 Hz, 3H) (Fig. S1, ESI†). IR (cm^{-1}): 3420 (b), 2962 (m), 2885 (m), 1705 (s), 1628 (w), 1492 (w), 1460 (m), 1419 (w), 1383 (w), 1363 (m), 1337 (sh), 1329 (w), 1223 (m), 1192 (w), 1097 (s), 1056 (s), 991 (s), 945 (w), 933 (w), 888 (w), 843 (s), 792 (m), 755 (w), 702 (m), 579 (m)) (Fig. S5, ESI†). Calculated elemental analysis: C, 45.97%; H, 8.14%; N, 11.91%. Found: C, 45.22%; H, 8.24%; N, 11.64%.

2.2.2 Synthesis of submicrometric particles of $[Cu_4I_6(pr\text{-}ted)_2]$. This synthesis has been carried out following a method previously described.[35] 2 g of PVP K90 are first dissolved in 200 mL of ethanol. 4 mL of a saturated water solution of KI is prepared and used to dissolve 0.38 g (3.5 mmol) of CuI. The CuI/KI solution is added dropwise to the solution of PVP in ethanol, which is then left to stir overnight. 0.32 g (2.5 mmol) of pr-ted are dissolved in 4 mL of ethanol and added dropwise to the flask containing CuI/KI/PVP. The content of the flask becomes turbid instantly exhibiting a white colour under visible light and green emission under UV light with λ_{exc} 365 nm. The suspension formed is washed once with water and twice with ethanol by centrifugation at 4500 rpm for 30 minutes. The submicrometric particles formed are resuspended in ethanol. IR (cm^{-1}): 3026 (w), 2997 (w), 2973 (w), 2928 (w), 2889 (w), 1672 (m), 1483 (w), 1468 (m), 1459 (s), 1444 (m), 1377 (s), 1359 (m), 1345 (w), 1321 (s), 1288 (m), 1095 (m), 1060 (w), 1048 (m), 1031 (m), 1009 (s), 981 (w), 948 (w), 936 (w), 890 (m), 842 (s), 809 (m), 794 (s), 776 (s), 756 (m), 712 (m), 687 (w), 660 (w), 647 (w), 628 (w), 617 (m). The PXRD spectrum shows a match with the phase obtained by single crystal X-ray diffraction. Found elemental analysis: $[Cu_4I_6(pr\text{-}ted)_2](PVP)_{0.6}$ C, 18.53%; H, 3.18%; N, 4.61%.

2.3 Water stability studies of submicrometric $[Cu_4I_6(pr\text{-}ted)_2]$ particles as a function of time (a) and pH (b)

(a) 5 mg of the submicrometric particles are dispersed in 5 mL of deionized water using magnetic stirring (800 rpm) for 5 days. The resulting suspension is centrifuged at 3600 rpm for 10 minutes, and the solid obtained is dried under vacuum.

0.6 mg of the dry submicrometric particles are dispersed in 0.6 mL of D_2O at room temperature using magnetic stirring for a few minutes. The ^{1}H-NMR spectra of the resulting suspensions are recorded over time from t_1 = 0 to t_{final} = 7 days.

(b) In three different vials, 5 mg of the submicrometric particles are dispersed in 5 mL of deionized water using magnetic stirring (800 rpm) for 30 minutes. To these vials, 1 mL of NaOH (0.01 M) is added until pH = 8.9, 2 mL of NaOH (0.01 M) until pH = 9.7, and 0.5 mL of HI (0.01 M) until pH = 4.2, respectively. Once the pH values are stabilized, the suspensions are centrifuged (3600 rpm) for 10 minutes to isolate the solids, which are then dried under vacuum. All the solids obtained are characterized using ATR-IR and PXRD.

2.4 Antibiotic detection experiments

All experiments have been performed according to the previously reported procedure.[38] The ability of submicrometric $[Cu_4I_6(pr\text{-}ted)_2]$ particles to detect various commonly used antibiotics such as SMZ, PAC, TC, and ORN, has been studied using deionized water and also with water collected from the Manzanares river at coordinates 40.750310°N, −3.894910°W, in the municipality of Manzanares del Real (postal code: 28410), Madrid, Spain. The general procedure for both waters is the same. 5 mg of submicrometric $[Cu_4I_6(pr\text{-}ted)_2]$ particles have been dispersed in 5 mL of water. By subjecting these suspensions to ultrasonic conditions (24 °C, 78 W), for 30 seconds, homogeneous and stable suspensions are obtained before carrying out measurements. To perform these experiments, 0.80 μmol of the antibiotics in aqueous solutions are added to the respective suspensions (concentration 400 μM for TC and 10^{-3} M for SMZ, CAP, and ORN). The emission spectra of submicrometric $[Cu_4I_6(pr\text{-}ted)_2]$ particles are obtained after allowing the species to react for 1 minute and exciting with a wavelength of 380 nm.

To study the TC detection capability of submicrometric $[Cu_4I_6(pr\text{-}ted)_2]$ particle suspensions have been prepared as described above. To perform this experiment, different volumes of an aqueous TC solution (400 μM) were progressively added to the corresponding suspension, obtaining the emission spectra of submicrometric $[Cu_4I_6(pr\text{-}ted)_2]$ particles for each addition. In this way, the aim is to study the reduction of the emission intensity of this compound according to the volume of added TC.

For the study of the submicrometric $[Cu_4I_6(pr\text{-}ted)_2]$ particles' selectivity to TC, suspensions of this compound have been prepared under the same conditions already described. To these suspensions, 0.80 μmol of the possible interfering antibiotics in aqueous solution were added (concentration 10^{-3}M for SMZ, CAP, and ORN), obtaining the emission spectrum of $[Cu_4I_6(pr\text{-}ted)_2]$ submicrometric particles in the presence of each antibiotic. A further 0.80 μmol of TC (400 μM) is then added to these suspensions, recording again the emission spectrum of submicrometric $[Cu_4I_6(pr\text{-}ted)_2]$ particles. Thus, it is possible to assess whether the presence of other antibiotics interferes with the detection of TC.

2.5 Recyclability

All recyclability experiments have been performed according to the previously reported procedure.[38] Aqueous suspension of submicrometric $[Cu_4I_6(pr\text{-}ted)_2]$ particles are prepared following the same procedure described in antibiotic detection experiments. To this suspension, 3 mL of an aqueous TC solution (400 μM) is added. After allowing the species to react for 5 minutes, the solution is centrifuged at 5000 rpm for 10 minutes. The supernatant is discarded, and the solid is washed with 2 portions of 5 mL of deionized water to remove the traces of TC. The resulting solid is suspended again in deionized water under the conditions described above and 3 mL of an aqueous TC solution (400 μM) is added. This experiment has been performed by repeating this process 30 times.

2.6 $[Cu_4I_6(pr\text{-}ted)_2]$ pellets

10 milligrams of the submicrometric $[Cu_4I_6(pr\text{-}ted)_2]$ particles are introduced inside a pressing die with a 3 mm diameter adapter and uniaxial pressure of 11.1 GPa is applied for 10 minutes forming circular pressed pellets of the solid.

2.7 $[Cu_4I_6(pr\text{-}ted)_2]$ in paper strips and glass fiber

The preparation of paper strips and glass fiber has been carried out following a previously reported procedure.[38] For each material (paper strips and glass-fiber respectively), two homogeneous suspensions are prepared by dispersing 5 mg of the submicrometric $[Cu_4I_6(pr\text{-}ted)_2]$ particles in 5 mL of ethanol with the help of ultrasonic bath sonication for 1 minute (24 °C, 60% power). Then the filter paper strips, and glass-fiber (2×4 cm^2 and 2.5×2.5 cm^2 size) respectively are immersed in each suspension for 30 minutes. Finally, both the paper strips and the glass fabric are removed from the suspensions and dried at room temperature for 1 hour.

2.8 Polylactic acid (PLA) composite sheets: $[Cu_4I_6(pr\text{-}ted)_2]$@PLA1%

0.08 g of PLA is introduced into a vial and dissolved in 2 mL of chloroform, under magnetic agitation (800 rpm) for 24 hours. Then, 0.8 mg of submicrometric $[Cu_4I_6(pr\text{-}ted)_2]$ particles are added obtaining a homogeneous suspension after 10 minutes under magnetic stirring and 10 minutes of sonication in an ultrasonic bath (24 °C, 68% power). Finally, 1 mL of this suspension is drop-casted on several 2.5×2.5 cm^2 glass surfaces. These surfaces are left at room temperature for 24 hours to let the solvent evaporate.

2.9 Commercial resin for 3D printing: $[Cu_4I_6(pr\text{-}ted)_2]$@mesh0.1%

Initially, a 5×5 cm^2 mesh with a thickness of 1 mm and a 1% concentration of submicrometric $[Cu_4I_6(pr\text{-}ted)_2]$ particles was fabricated. However, it was demonstrated that reducing the concentration to 0.1% not only decreases the consumption of the compound, thereby lowering costs, but also produces a material that effectively functions as a TC sensor. To prepare the same size mesh with this optimized composition ($[Cu_4I_6(pr\text{-}ted)_2]$@mesh0.1%), 3 mL of standard commercial resin were mixed in a vial with 0.5 mL of a suspension of submicrometric $[Cu_4I_6(pr\text{-}ted)_2]$ particles in EtOH with a concentration of 6.33 mg mL^{-1}. This mixture was subjected to sonication in an ultrasonic bath at 60% power for 10 minutes. After sonication, the resulting mixture was transferred into the 3D printing

tank. Similar conditions and procedures allow printing objects with different morphologies.

3. Results and discussion

3.1 Submicrometric $[Cu_4I_6(pr\text{-}ted)_2]$ particles

The synthesis of the spherical submicrometric particles with a solid average size of 369.2 ± 129.5 nm as indicated by SEM (Fig. 1b and Fig. S3, ESI†), was carried out following a previously published method[35] by reacting a saturated aqueous solution of KI and CuI with a polyvinylpyrrolidone (PVP) solution in ethanol using magnetic stirring at room temperature for 12 hours. The pr-ted ligand is added at the end forming the desired suspension instantly. After centrifugation, washing, and air drying, their PXRD diffraction pattern was recorded, and it could be seen that it matches with the simulated powder pattern of $[Cu_4I_6(pr\text{-}ted)_2]$, elucidated previously by single crystal X-ray diffraction (Fig. 1a and Fig. S4, ESI†) indicating the presence of same crystalline phase corresponding to a molecular crystal with a purely inorganic anionic part $[Cu_4I_6]^{2-}$ and a cationic part constituted by the organic ligands (pr-ted) connected to each other by coordination bonds between the nitrogen atoms of the two $[pr\text{-}ted]^+$ ligands and the Cu(I) atoms (Fig. 1a).[50]

Additionally, their ATR-FTIR spectrum corresponds to the expected $[Cu_4I_6(pr\text{-}ted)_2]$ compound, showing a band around 1670 cm^{-1} attributed to the stretching vibration of the carbonyl group of PVP (Fig. S5, ESI†). The elemental analysis is also consistent with the existence of a small proportion of PVP. Nonetheless, the presence of PVP with the compound does not affect the conducted TC detection.

The study of the hydrodynamic radius of $[Cu_4I_6(pr\text{-}ted)_2]$ particles using DLS shows that the particles suspended in ethanol have an average radius of 495.2 nm, while the particles suspended in water have an average radius of 841.0 nm (Fig. 1c and Table S1, ESI†).

3.2 Water stability of submicrometric $[Cu_4I_6(pr\text{-}ted)_2]$ particles

To use the submicrometric $[Cu_4I_6(pr\text{-}ted)_2]$ particles as a luminescent sensor for antibiotics in water, they must be stable in water across a broad pH spectrum and during the time of use. This stability is crucial to prevent the compound from breaking down into its constituent elements or forming additional compounds, thereby avoiding secondary contamination of the water. Fig. 2 shows the PXRD diffraction patterns and ATR-FTIR spectra of the submicrometric particles after being immersed in water at room temperature for 7 days (Fig. 2a and c; red lines) and 30 minutes at pHs between 4.3 and 8.9 (Fig. 2b and d; red, blue and green lines), which is consistent with the wastewater pH range of 4.50–10.0.

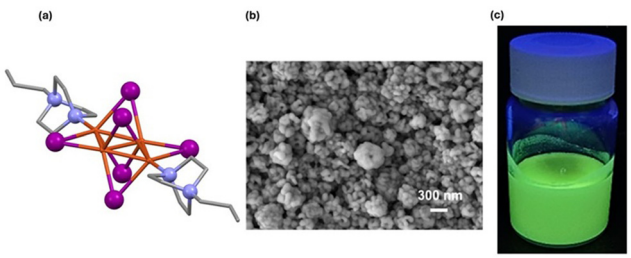

Fig. 1 Image of the structure of $[Cu_4I_6(pr\text{-}ted)_2]$. The Cu atoms are represented in orange, iodine atoms in violet, and nitrogen atoms in blue. Hydrogen atoms have been omitted for clarity (a). SEM image of submicrometric $[Cu_4I_6(pr\text{-}ted)_2]$ particles (b). Image of submicrometric $[Cu_4I_6(pr\text{-}ted)_2]$ particles suspended in ethanol, under ultraviolet light (λ = 365 nm) (c).

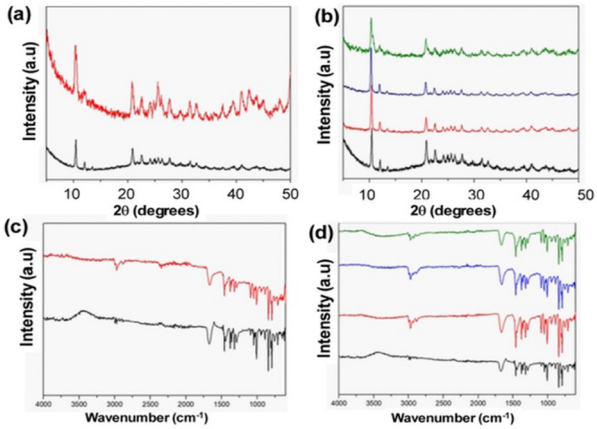

Fig. 2 PXRD diffraction pattern and ATR-FTIR spectra of submicrometric $[Cu_4I_6(pr\text{-}ted)_2]$ particles (black), compared with the results of the diffraction pattern of the compound after being immersed in water for 7 days (red) (a) and (c). PXRD diffraction pattern, and ATR-FTIR of submicrometric $[Cu_4I_6(pr\text{-}ted)_2]$ particles (black), compared with the compound after being immersed in water at pH = 4.30 (red), pH = 7.30 (blue) and pH = 8.90 (green) (b) and (d).

As specified by Spanish normative RD 3/2023 (BOE Royal Decree 3/2023, dated January 10, which prescribes the technical-sanitary criteria for the quality, control, and supply of drinking water, BOE number 9, January 10, 2023, pages 4253–4354). When these spectra are compared to those of submicrometric $[Cu_4I_6(pr\text{-}ted)_2]$ particles (Fig. 2, black lines) it can be said that under all conditions studied, the submicrometric particles maintain their chemical nature intact, confirming the compound's stability in water.

However, ^{1}H-NMR studies of submicrometric $[Cu_4I_6(pr\text{-}ted)_2]$ particles in D_2O over time (from time 0 to 7 days) show us that a small part of the compound initially dissociates into the starting ligand, without continuing its degradation over time (Fig. S6, ESI†). This leads us to eliminate the direct use of the compound as a chemical sensor in water and encourages us to process it in more stable and robust devices.

3.3 Sensing *versus* TC

To evaluate the antibiotic detection capabilities of submicrometric $[Cu_4I_6(pr\text{-}ted)_2]$ particles, four antibiotics from different commonly used antibiotic families were chosen: sulfonamides, chloramphenicols, tetracyclines, and nitroimidazoles. As illustrated in Fig. 3b, the emission intensities of the aqueous suspension of submicrometric $[Cu_4I_6(pr\text{-}ted)_2]$ particles remain

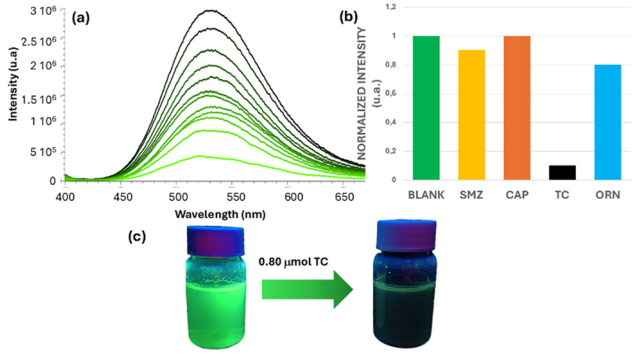

Fig. 3 Emission spectrum of an aqueous suspension of submicrometric $[Cu_4I_6(pr\text{-}ted)_2]$ particles as a function of the concentration of different added TC solutions (a). Normalized emission intensity of the aqueous suspension of $[Cu_4I_6(pr\text{-}ted)_2]$ submicrometric particles (1 mg mL^{-1}) after reacting for 1 minute with 0.80 µmol of various commonly used antibiotics (b). Quenching of the bright green emission of $[Cu_4I_6(pr\text{-}ted)_2]$ submicrometric particles after adding 0.80 µmol of TC, under UV lamp ($\lambda_{exc.}$ = 365 nm) (c).

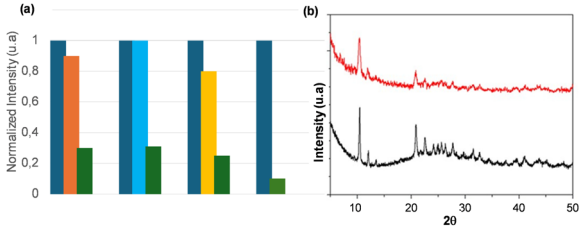

Fig. 4 (a) Normalized emission intensity of the aqueous suspension of submicrometric $[Cu_4I_6(pr\text{-}ted)_2]$ particles (1 mg mL^{-1}) after reacting for 1 minute with 0.80 µmol of various commonly used antibiotics. Dark blue bar (white), orange bar SMZ, blue bar CAP, yellow bar ORN, and dark green bar TC. Measurements were taken at room temperature. (b) PXRD diffraction pattern of submicrometric $[Cu_4I_6(pr\text{-}ted)_2]$ particles (black) and of the same particles after 30 cycles in the presence of TC (red).

largely unchanged after reacting for one minute with 0.80 µmol of SMZ, CAP, and ORN (10^{-3} M, 0.8 mL). In contrast, the suspension's emission intensity significantly diminishes after one minute of reacting with 0.80 µmol of TC (400 µM, 2.1 mL). These findings indicate that TC can be detected instantaneously in aquatic environments, rendering the compound effective as a real-time luminescent sensor for TC detection.

The interaction of submicrometric $[Cu_4I_6(pr\text{-}ted)_2]$ particles with TC was investigated by examining the relationship between the emission intensity of the compound and the concentration of TC in deionized (Fig. 3, and Fig. S8, ESI†) and real river water (Fig. S9, ESI†) respectively. As shown in Fig. 3a, an increase in the TC concentration in the medium results in a corresponding decrease in the emission intensity of the aqueous suspension of submicron $[Cu_4I_6(pr\text{-}ted)_2]$ particles transitioning from a bright green emission to almost no emission.

The linear correlation between the emission intensity of the aqueous suspensions and the TC concentration was analyzed using the Stern–Volmer (S–V) equation.[51] The S–V plots show a high linear correlation in the TC concentration range of 0–2.5 µM (R^2 = 0.9911/R^2 = 0.9927) (Fig. S8 and S9, ESI†). The calculated K_{sv} values are 4.35 10^4 M^{-1} (deionized water) and 4.11 10^4 M^{-1} (river water) respectively, and the limit of detection (LOD) values, determined according to the IUPAC criterion[52] (3σ/slope), where $\sigma = 100 \times (S/I_0)$ and S is the standard deviation of $(I_0 - I)/I_0$ are 1.18 nM and 1.9 nM, respectively. These LODs are significantly lower than the maximum TC concentration permitted in milk by the European Union,[42,53] and would allow the detection of quantities of tetracycline below the amounts normally present in water.

3.4 Sensor selectivity and recyclability

Beyond stability and sensitivity, selectivity for the target analyte is a vital aspect in the development of a luminescent sensor. In this context, the potential for interference by other commonly used antibiotics in the detection of TC in water has been examined, including SMZ, CAP, and ORN. As depicted in Fig. 4, the emission intensity of the aqueous suspension of submicrometric $[Cu_4I_6(pr\text{-}ted)_2]$ particles remains largely unchanged after a one-minute reaction with 0.80 µmol of SMZ, CAP, and ORN. However, the addition of 0.80 µmol of TC to these suspensions results in a significant decrease in emission intensity. This reduction in emission intensity is comparable to that observed when these potential interfering substances are absent. The findings confirm that $[Cu_4I_6(pr\text{-}ted)_2]$ can effectively detect TC even in the presence of other prevalent drugs.

Additionally, the recyclability of submicrometric $[Cu_4I_6(pr\text{-}ted)_2]$ particles following exposure to TC over 30 cycles has been assessed. After subjecting the particles to this number of cycles, both the PXRD diffraction pattern (Fig. 4b) and ATR-FTIR spectra (Fig. S10, ESI†) exhibit the expected signals associated with compound $[Cu_4I_6(pr\text{-}ted)_2]$, indicating that this compound can be used several consecutive times in TC detection tests.

The data obtained for K_{SV}, LOD, and cycle count are found to be quite relevant when compared with similar studies performed with other coordination compounds (Table 1). Previously published compounds usually show a low cycle count and higher LOD values (Table 1). It should also be mentioned that most of the published coordination compounds require synthesis with long reaction times, high temperatures, and pressures. Consequently, the findings confirm that submicrometric $[Cu_4I_6(pr\text{-}ted)_2]$ particles are an exceptionally selective sensor for detecting TC in water.

3.5 Fluorescence quenching mechanism to TC

If an appropriate energy level alignment between the electronically excited state of the fluorescent compound and the analyte exists, an electron transfer from the fluorescent material to the analyte can occur. This process, known as the photoinduced electron transfer (PET) effect, results in fluorescence quenching.[43]

Table S2 (ESI†) provides the HOMO (highest occupied molecular orbital) and LUMO (lowest unoccupied molecular orbital) energy levels of TC calculated using the density functional theory (DFT) method. These values are consistent with previous studies.[43] The predicted HOMO–LUMO gap of TC is 3.49 eV, which is close to the theoretical band gap of

$[Cu_4I_6(pr\text{-}ted)_2]$, measured "3.20 eV" (as shown in Fig. S11, ESI†), in very good agreement with the experimental excitation energy. The electron transfer between the donor material and the acceptor TC prevents the excitation electron from returning to the ground state. On the other hand, when the excitation and/or emission light of the fluorescent material is absorbed by the analyte, the fluorescence inner filter effect (IFE) happens. The absorption spectrum of TC has a maximum in the visible region at 357–360 nm (in water solutions),[40] while the fluorescence excitation of $[Cu_4I_6(pr\text{-}ted)_2]$ particles in aqueous solution has a maximum at 380 nm and an emission at 530 nm (Fig. S12, ESI†). It is evident that the absorption peak of TC does not overlap with the emission peak of $[Cu_4I_6(pr\text{-}ted)_2]$ particles.[54] This suggests that TC does not significantly absorb the emission light of $[Cu_4I_6(pr\text{-}ted)_2]$ particles, thereby reinforcing the hypothesis of a resonant electron transfer between material and TC.

3.6 Low-cost, robust, and portable devices

The submicrometric particles and their stable water/ethanol suspensions facilitate their processing by applying different simple techniques.[55] Indeed, the submicrometric particles water suspension can be easily attached by immersion (dip-coating) to paper fibers forming paper strips (Fig. 5b and 6a and b), which is one of the most referenced devices in scientific literature.[56] However, due to the general poor reusability of these paper strip-based devices, we have also developed a portable device with a different morphology based on fiberglass (Fig. 5a and 6c and d). Additionally, sensitive composite sheets and meshes have been created using polylactic acid (PLA) as a biodegradable polymer matrix and commercial resins through drop casting, and 3D printing technology (Fig. 5c and d and 6e, f, i and j) respectively. Finally, the submicrometric particles have been pressed by uniaxial pressure (11.1 GPa) forming highly emissive and robust pellets (Fig. 6g and h and Fig. S13, ESI†).

In all cases, the original emission intensity remains very high, even despite only adding a small amount of compound in the formation of the composite with PLA (1%) and in the doping of the commercial resin (1% and 0.1%), thanks to the compound's high quantum yield (close to 100%) (Fig. 6). The emission spectra show the original emission of the compound at 530 nm (Fig. S12 and S14, ESI†), except for the pressed pellet that suffers a slight bathochromic shift towards 550 nm (Fig. S15, ESI†). In this case, the PXRD diffraction pattern indicates that after exerting 11.1 GPa of uniaxial pressure the compound maintains its initial crystalline phase (Fig. S16, ESI†). Moreover, in the case of $[Cu_4I_6(pr\text{-}ted)_2]$@PLA1% and $[Cu_4I_6(pr\text{-}ted)_2]$@mesh1%, the PXRD diffractograms (Fig. S18 and S19, ESI†) of both materials show that after their formation the compound $[Cu_4I_6(pr\text{-}ted)_2]$ present as doping agent maintains its initial structure. In addition, all the devices have been studied by SEM-EDX, and the SEM images generated show a homogeneous distribution of the submicrometric particles on the paper strips, on the glass fibers, PLA sheets ($[Cu_4I_6(pr\text{-}ted)_2]$@PLA1%), and in the mesh with commercial resin ($[Cu_4I_6(pr\text{-}ted)_2]$@resin0.1%) (Fig. S20–S25, ESI†). As shown in Fig. 6, the emission intensity of all devices remains unchanged in the presence of 5 mL of water, while instantaneity quenches in the presence of 5 mL of an aqueous TC (400 μM) solution. Additionally, the degree of quenching can be visually appreciated at different concentrations of TC (Fig. S26, ESI†).

The devices respond instantaneously to the presence of TC, which attenuates their emission. All of them can be immersed in water contaminated with TC (400 μM) at least 30 times without losing their ability to act as sensors. The ^{1}H-NMR spectra of D_2O exposed to 30 immersions of the different devices do not show signs of their possible water degradation (Fig. 7).

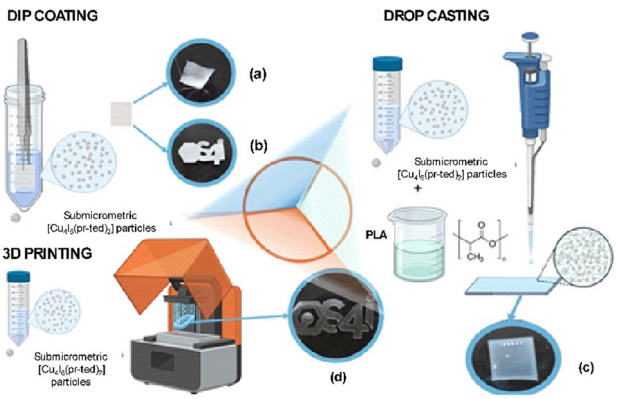

Fig. 5 Preparation diagram of the different composites using submicrometric $[Cu_4I_6(pr\text{-}ted)_2]$ particles. Dip coating to obtain the fiberglass (a) and paper strips (b). Drop casting to obtain the composite with PLA $[Cu_4I_6(pr\text{-}ted)_2]$@PLA1%, (c). 3D printing to obtain the composite $[Cu_4I_6(pr\text{-}ted)_2]$@mesh0.1% (d).

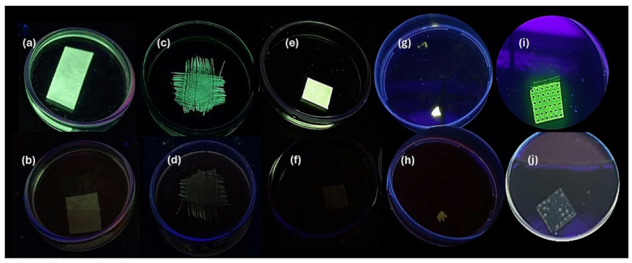

Fig. 6 Emission intensity of paper strips (a) and (b), and fiberglass (c) and (d) impregnated with sub-micrometric $[Cu_4I_6(pr\text{-}ted)_2]$ particles. $[Cu_4I_6(pr\text{-}ted)_2]$@PLA1% (e) and (f), pressed pellets (g) and (h), and $[Cu_4I_6(pr\text{-}ted)_2]$@mesh0.1% (3D printed) (i) and (j). All of them in 5 mL of water (a), (c), (e), (g), and (i) and after immersing them in 5 mL water with TC (400 μM) (b), (d), (f), (h), and (j). Under UV light ($\lambda_{exc.}$ = 365 nm).

4. Conclusions

The investigated compound demonstrates optimal properties for use as a chemical sensor, exhibiting a highly efficient and rapid response in detecting tetracycline in real water samples. The obtained limit of detection (LOD) value of 1.18 nM indicates a high sensitivity to tetracycline. Additionally, the compound's reusability was confirmed through 30 cycles in

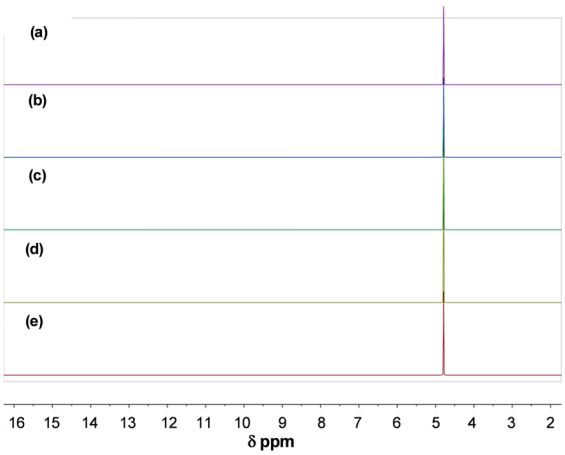

Fig. 7 ^{1}H-NMR spectra after submerging the pellets (a), the $[Cu_4I_6(pr\text{-}ted)_2]$@mesh0.1% (b), the coated paper strips (c), $[Cu_4I_6(pr\text{-}ted)_2]$@PLA1% (d), and the coated fiberglass (e), respectively, into D_2O 30 times (one minute each time).

this study, highlighting its durability. These findings are particularly significant when compared to previous studies using other types of luminescent compounds.

Notably, the synthesis of this compound is performed at room temperature in a water/ethanol mixture in a single step, which facilitates scalability. A crucial aspect of this work is the submicrometric size of the compound, allowing for the creation of stable suspensions in water and ethanol, essential for material processing, and preventing the decomposition of the submicroparticles in water. This is a significant advancement, as processing has been poorly carried out in published studies on sensors with turn-off responses.

This research enables the development of various devices, including paper strips, glass fiber, PLA composite strips, and even 3D-printed grids, using a minimal amount of compound. Indeed, the 3D printing of grids is achieved with commercial resins containing just 0.1% of the compound. These devices are inexpensive, sensitive, easy to handle, reusable, and portable, making them highly practical for industrial-level detection of TC in real water samples.

Abbreviations

ATR-FTIR	Attenuated total reflectance Fourier-transform infrared
CAP	Chloramphenicol
CC	Cluster-centered
DFT	Density functional theory
DLS	Dynamic light scattering
LOD	Limit of detection
MLCT	Metal-to-ligand charge transfer
ORN	Ornidazole
PAW	Projected augmented wave
PBC	Periodic boundary conditions
PLA	Polylactic acid
pr-ted	1-Propyl-1,4-diazabicyclo[2.2.2]octan-1-ium
PVP	Polyvinylpyrrolidone
PXRD	X-ray powder diffraction
SEM	Scanning electron microscopy
SEM-EDX	Scanning electron microscopy with energy dispersive X-ray spectroscopy
SMZ	Sulfamethazine
S–V	Stern–Volmer
TC	Tetracycline
Ted	Triethylenediamine
TGA	Thermogravimetric analysis
VASP	Vienna *ab initio* simulation package

Author contributions

The manuscript was written with contributions from all authors. All authors have approved the final version of the manuscript. P. A. O.: conceptualization. E. R.: methodology. R. G., G. L. and A. G. H.: methodology, writing – review and editing. F. A.: formal analysis, software. P. A. O.: investigation and contributed to formal analysis. P. A. O.: funding acquisition, resources, project administration, supervision, writing – original draft, writing – review, and editing.

Data availability

The data supporting this article have been included as part of the ESI.†

Conflicts of interest

There are no conflicts to declare. The authors declare that they have no known competing financial interests or personal relationships that could have appeared to influence the work reported in this paper.

Acknowledgements

This work was supported by MCINN/AEI/10.13039/5011000011033 and European Union Next Generation EU/PRTR, under the National Program of Sciences and Technological Materials (PID2022–138968NB-C21, PID2022–138968NB-C22, and PID2022-138470NB-I00). The authors thank Marta Muñoz from URJC for her help in processing the materials. This work is dedicated to Juan Jesús Amo Mora.

References

1 M. Murillo, J. Alvarez-Conde, R. Wannemacher, J. Cabanillas-Gonzalez, J. Gonzalez-Platas, U. R. Rodriguez-Mendoza, A. Liang, R. Turnbull, D. Errandonea, J. Ignacio Martinez and P. Amo-Ochoa, *J. Mater. Chem. C*, 2022, **10**, 18004.
2 J. Conesa-Egea, J. Gallardo-Martinez, S. Delgado, J. I. Martinez, J. Gonzalez-Platas, V. Fernandez-Moreira, U. R. Rodriguez-Mendoza, P. Ocon, F. Zamora and P. Amo-Ochoa, *Small*, 2017, **13**, 1700965.

3 Q. Benito, B. Baptiste, A. Polian, L. Delbes, L. Martinelli, T. Gacoin, J.-P. Boilot and S. Perruchas, *Inorg. Chem.*, 2015, **54**, 9821.
4 M. Gavrilescu, K. Demnerova, J. Aamand, S. Agathoss and F. Fava, *New Biotechnol.*, 2015, **32**, 147.
5 X. Qu, P. J. J. Alvarez and Q. Li, *Water Res.*, 2013, **47**, 3931.
6 X. Wu, X.-X. Chen and Y.-B. Jiang, *Analyst*, 2017, **142**, 1403.
7 T. Becker, S. Mühlberger, C. Bosch-von Braunmühl, G. Müller, T. Ziemann and K. V. Hechtenberg, *Sens. Actuators, B*, 2000, **69**, 108.
8 H. Qi, M. Teng, M. Liu, S. Liu, J. Li, H. Yu, C. Teng, Z. Huang, H. Liu, Q. Shao, A. Umar, T. Ding, Q. Gao and Z. Guo, *J. Colloid Interface Sci.*, 2019, **539**, 332.
9 X.-D. Zhu, K. Zhang, Y. Wang, W.-W. Long, R.-J. Sa, T.-F. Liu and J. Lu, *Inorg. Chem.*, 2018, **57**, 1060–1065.
10 L. Ma, M. Petersen and X. Lu, *Appl. Environ. Microbiol.*, 2020, **86**(9), e00096-20.
11 K. Wang, Y. Dong, X. Zhao, X. Bai, L. Li, J. Guo, Z. Wang, H. Tang and Y. Ma, *J. Mol. Struct.*, 2024, **1295**, 136725.
12 G.-L. Wang, M.-L. Wang, W. Zhong, M. Afzal, A. Alarifi, S. Singh, A. Kumar and J. Jin, *J. Mol. Struct.*, 2022, **1264**, 133332.
13 J. Troyano, J. Perles, P. Amo-Ochoa, J. I. Martínez, F. Zamora and S. Delgado, *CrystEngComm*, 2014, **16**, 8224.
14 K. Hassanein, P. Amo-Ochoa, C. J. Gomez-Garcia, S. Delgado, O. Castillo, P. Ocon, J. I. Martinez, J. Perles and F. Zamora, *Inorg. Chem.*, 2015, **54**, 10738.
15 P. Amo-Ochoa, K. Hassanein, C. J. Gomez-Garcia, S. Benmansour, J. Perles, O. Castillo, J. I. Martinez, P. Ocon and F. Zamora, *Chem. Commun.*, 2015, **51**, 14306.
16 K. Hassanein, J. Conesa-Egea, S. Delgado, O. Castillo, S. Benmansour, J. I. Martínez, G. Abellan, C. J. Gómez-García, F. Zamora and P. Amo-Ochoa, *Chem. – Eur. J.*, 2015, **21**, 17282.
17 J. P. Leonard, C. B. Nolan, F. Stomeo and T. Gunnlaugsson, Photochemistry and Photophysics of Coordination Compounds: Lanthanides, in *Photochemistry and Photophysics of Coordination Compounds II*, ed. V. Balzani and S. Campagna, Topics in Current Chemistry, Springer, Berlin, Heidelberg, 2007, vol. 281.
18 L. Feng, J. Pang, P. She, J.-L. Li, J.-S. Qin, D.-Y. Du and H.-C. Zhou, *Adv. Mater.*, 2020, **32**, 2004414.
19 X. Zhang, L. Zhang, H. Bie, J. Xu, Y. Yuan and L. Jia, *Spectrochim. Acta, Part A*, 2023, **299**, 1228678.
20 M. Miao, L. Mu, S. Cao, Y. Yang and X. Feng, *Carbohydr. Polym.*, 2022, **291**, 119587.
21 S. Mondal and D. Sarma, *Soft Matter*, 2023, **19**, 4926.
22 D. B. Kanzariya, R. Goswami, D. Muthukumar, R. S. Pillai and T. K. Pal, *ACS Appl. Mater. Interfaces*, 2022, **14**, 86581.
23 R. Goswami, S. C. Mandal, B. Pathak and S. Neogi, *ACS Appl. Mater. Interfaces*, 2019, **11**, 9042.
24 C. Li, X. Sun, X. Meng, D. Wang and C. Zheng, *Dalton Trans.*, 2023, **52**, 7611.
25 Y. Zhou, Q. Yang, D. Zhang, N. Gan, Q. Li and J. Cuan, *Sens. Actuators, B*, 2018, **262**, 137.
26 O. Caballero-Calero, J. R. Ares and M. Martin-Gonzalez, *Adv. Sustainable Syst.*, 2021, **5**, 2100095.
27 L. M. Peter, *Philos. Trans. R. Soc., A*, 2011, **369**, 1840.
28 K. Binnemans, P. T. Jones, B. Blanpain, T. Van Gerven and Y. Pontikes, *J. Cleaner Prod.*, 2015, **99**, 17.
29 M. Murillo, A. García, J. López, J. Perles, I. Brito and P. Amo-Ochoa, *Catal. Today*, 2023, **418**, 114072.
30 A. Kobayashi and M. Kato, *Chem. Lett.*, 2017, **46**, 154.
31 S. Perruchas, *Dalton Trans.*, 2021, **50**, 12031.
32 X.-C. Shan, F.-L. Jiang, L. Chen, M.-Y. Wu, J. Pan, X.-Y. Wan and M.-C. Hong, *J. Mater. Chem. C*, 2013, **1**, 4339.
33 E. Cariati, E. Lucenti, C. Botta, U. Giovanella, D. Marinotto and S. Righetto, *Coord. Chem. Rev.*, 2016, **306**(Part 2), 566.
34 D. V. Scaltrito, D. W. Thompson, J. A. O'Callaghan and G. J. Meyer, *Coord. Chem. Rev.*, 2000, **208**, 243.
35 J.-J. Wang, C. Chen, W.-G. Chen, J.-S. Yao, J.-N. Yang, K.-H. Wang, Y.-C. Yin, M.-M. Yao, L.-Z. Feng, C. Ma, F.-J. Fan and H.-B. Yao, *J. Am. Chem. Soc.*, 2020, **142**, 3686.
36 Y. Fang, W. Liu, S. J. Teat, G. Dey, Z. Shen, L. An, D. Yu, L. Wang, D. M. O'Carroll and J. Li, *Adv. Funct. Mater.*, 2017, **27**, 1603444.
37 X. Hei and J. Li, *Chem. Sci.*, 2021, **12**, 3805.
38 C. Li, C. Zeng, Z. Chen, Y. Jiang, H. Yao, Y. Yang and W.-T. Wong, *J. Hazard. Mater.*, 2020, **384**, 121498.
39 Y. Zhao, M. Liu, S. Zhou, Z. Yan, J. Tian, Q. Zhang and Z. Yao, *Food Chem.*, 2023, **425**, 136449.
40 F. Sun, H.-H. Xie, X. Liu, S. Pang, S.-F. Tang and X. Xu, *J. Solid State Chem.*, 2023, **322**, 123942.
41 Y. Li, Y. Wang, P. Du, L. Zhang, Y. Liu and X. Lu, *Sens. Actuators, B*, 2022, **358**, 131526.
42 P. Zhang, X. Li and Y. Xu, *New J. Chem.*, 2022, **46**, 13129.
43 M.-L. Zhang, X.-Y. Lu, Y. Bai, Y.-X. Ren, J.-J. Wang and X.-G. Yang, *Dyes Pigm.*, 2022, **202**, 110172.
44 C. Fan, X. Zhang, C. Xu, R. Wu, N. Li, L. Wang, D. Zhang, S. Bi and Y. Fan, *Inorg. Chim. Acta*, 2020, **509**, 119665.
45 G.-N. Liu, R.-D. Xu, R.-Y. Zhao, Y. Sun, Q.-B. Bo, Z.-Y. Duan, Y.-H. Li, Y.-Y. Wang, Q. Wu and C. Li, *ACS Sustainable Chem. Eng.*, 2019, **7**, 18863.
46 G. Kresse and J. Hafner, *Phys. Rev. B: Condens. Matter Mater. Phys.*, 1993, **47**, 558.
47 G. Román-Pérez and J. M. Soler, *Phys. Rev. Lett.*, 2009, **103**, 096102.
48 J. Klimeš, D. R. Bowler and A. Michaelides, *J. Phys.: Condens. Matter.*, 2010, **22**, 022201.
49 A. V. Krukau, O. A. Vydrov, A. F. Izmaylov and G. E. Scuseria, *J. Chem. Phys.*, 2006, **125**, 22201.
50 W. Liu, K. Zhu, S. J. Teat, G. Dey, Z. Shen, L. Wang, D. M. O'Carroll and J. Li, *J. Am. Chem. Soc.*, 2017, **139**, 9281.
51 M. H. Gehlen, *J. Photochem. Photobiol., C*, 2020, **42**, 100338.
52 F. Allegrini and A. C. Olivieri, *Anal. Chem.*, 2014, **86**, 7858.
53 C. Robert, N. Gillard, P. Y. Brasseur, G. Pierret, N. Ralet, M. Dubois and P. Delahaut, *Food Addit. Contam., Part A: Chem., Anal.*, 2013, **30**, 443.
54 I. Bezruk, V. Vrakin, L. Savchenko, A. Materiienko and V. Georgiyants, *Scr. Sci. Pharm.*, 2017, **4**, 33.
55 V. G. Vegas, R. Lorca, A. Latorre, K. Hassanein, C. J. Gómez-García, O. Castillo, A. Somoza, F. Zamora and P. Amo-Ochoa, *Angew. Chem., Int. Ed.*, 2017, **56**, 987.
56 R. Sivakumar and N. Y. Lee, *Biochip J.*, 2021, **15**, 216.

